Momentum-transfer dispersion relations for electron-atom cross sections

D. Bessis,* A. Haffad, and A. Z. Msezane
Department of Physics and Center for Theoretical Studies of Physical Systems, Clark Atlanta University, Atlanta, Georgia 30314
(Received 24 August 1993)

We derive momentum-transfer dispersion relations by showing that at fixed impact energy the electron-atom differential cross sections are analytic functions of the momentum transfer squared K^2 in a complex plane cut from $-\infty$ to 0, along the real axis. It is therefore natural to introduce sets of interpolating rational functions of K^2 to fit experimental data. The most suitable are the Padé approximations. We find that the zeros and the poles of these approximations split into two families. One family is made of poles and zeros that sit on the cut, yielding a good simulation of it. The other family takes care of the noise in the data: poles and zeros appearing in *pairs* very near each other. We can therefore first filter the noise by eliminating those pairs. Among the remaining poles, one pole is extremely near $K^2=0$ for the inelastic differential cross sections. We apply this technique to recompute both elastic and inelastic cross sections for Xe, Kr, and Ar atoms, at impact energies of 100, 400, and 500 eV. In this way, we get the optical oscillator strength for two optically connected states. Our results are compared with other experimental as well as theoretical results.

PACS number(s): 32.70.Cs, 34.80.Dp, 34.90.+q

I. INTRODUCTION

Miller and Platzman [1] have pointed out that for $K^2 \ll 1$ the generalized oscillator strength (GOS) is constant and reduces to the optical oscillator strength (OOS). Lassettre, Skerbele, and Dillon [2] inferred that the GOS converges to the OOS as $K^2 \equiv t \to 0$ for inelastic electron transitions regardless of the applicability of the Born approximation and therefore at any impact energy. The limiting behavior of the GOS at $t=0$ is important in the normalization of the experimentally determined relative differential cross sections for excitation by electron impact [3–7], calculation of the cross sections for energy transfer [8], and in the determination of the OOS [9–11]. Also, it has been examined [7–9,12,13] with no clear departure from the limiting theorem. However, difficulties [13] and incompatibilities [14] with the limit theorem have been reported.

Because, for finite electron impact energy E, the value $t=0$ is unphysical, it is necessary to use an interpolation-extrapolation algorithm on the experimental data to reach it. In general, two different fitting procedures are used. For the elastic differential cross sections, one uses [9,15]

$$\left[\frac{d\sigma}{d\Omega}\right]_{\rm el} = \exp[C_0 + C_1 K + C_2 K^2 + C_3 K^3] , \tag{1}$$

which in the complex $t=K^2$ plane produces an approximation analytic in the plane cut along the negative real axis (square root branch point). We shall see that although this approximation has correct analytical structure, it can be greatly improved.

For dipole allowed transitions, most authors, following Lassettre, write an expansion for the GOS in the following form:

$$F(t) = \frac{1}{(t+t_0)^6}\left[f_0 + f_1 \frac{t}{t+t_0} + \cdots + f_n \left[\frac{t}{t+t_0}\right]^n\right] . \tag{2}$$

The power six in the first exponent is associated with the $s \to p$ transitions that we more specifically study in this paper. We shall see that $F(t)$ is analytic in the complex t plane cut from minus infinity to zero. A formula such as Eq. (2) represents $F(t)$ as the ratio of a polynomial of degree n to the polynomial $(t+t_0)^{n+6}$ that is by a rational fraction with a pole of order $(n+6)$ located at $t=-t_0$. The discontinuity of the cut has been replaced by a pole of high degree $(n+6)$. See Figs. 1(a) and 1(b). The two kinds of fitting procedures, Eq. (1) for the elastic cross sections and Eq. (2) for the GOS, suffer the same deficiency: those are *a priori* expansions, based on some modeling and/or intuition of the various authors who proposed them. The aim of this paper is to propose an unbiased method totally model-independent and based on axiomatic theory, that is on the analytic properties of the scattering amplitudes. In Sec. II, we derive the analytic properties of the GOS, as a function of the squared momentum transfer $t=K^2$, at fixed incoming electron impact energy E. In Sec. III, we introduce a general approximation

$$F_n(t) = \frac{P_n(t)}{Q_n(t)} , \tag{3}$$

where $P_n(t)$ and $Q_n(t)$ are polynomials (the subscript n

*Permanent address: Service de Physique Théorique CEN-Saclay, Gif-sur-Yvette 91191 France.

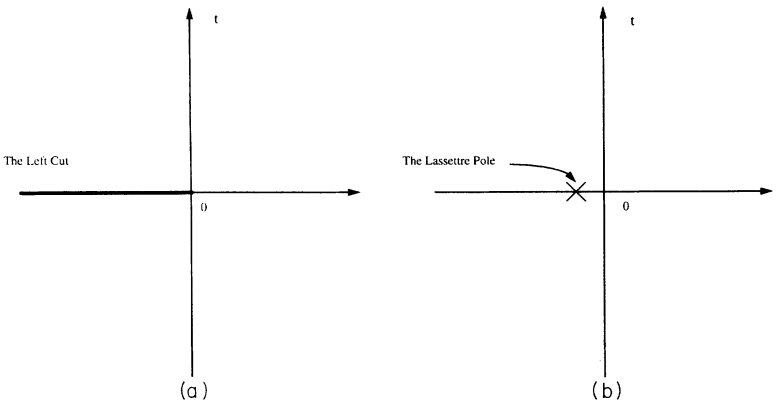

FIG. 1. Analytic properties of the generalized oscillator strength in the complex transfer plane. (a) represents the full cut; (b) shows the replacement of the full cut by a pole of order $(n+6)$ in the Lassettre approximation.

represents here a label characterizing the order of the approximation, and it is not the degree of those polynomials). In the Lassettre approximation, the denominator $Q_n(t)$ was $(t+t_0)^{n+6}$ while the numerator was adjusted to fit the data. In the method of Padé approximations, neither the numerator nor the denominator has a prescribed form. Both are optimized simultaneously to the data.

In Sec. IV A, we introduce those rational approximations using the continued fraction approach. We show that the numerators and the denominators of these approximations satisfy a three-term recursive relation that allows them to be found efficiently. In the literature, these approximations are known under the name of Padé approximants of type II [16,17]. In Sec. IV B, we analyze the distribution of the zeros and the poles of these Padé approximants in the complex transfer plane. We discover that these zeros and poles split very significantly into two families.

(a) A first family consisting of the "noisy" zeros and poles. These are generated by the existence of noise and/or the statistical character of the data. The Padé approximant plays the role of noise filter for an analytic function [18]. These zeros and poles are very easy to recognize; they always appear as a pair of extremely near zero pole (and therefore tend to compensate each other). The distance between the element of the pair being of the order of the noise.

(b) The second family is made up of zeros and poles sitting distant to each other on the left-hand cut (real negative axis). Clearly their role is to simulate the discontinuity on the cut. In Sec. V, we use the fact that the OOS is proportional to the residue of the pole at $t=0$ of the inelastic differential cross section to compute the OOS from the Padé approximation. Inspecting the poles left after getting rid of the first family of zeros and poles, we discover a unique pole extremely near zero, within the same distance to zero as the distance between a doublet pole zero representing the noise. The residue of this pole provides the OOS. The fact that the Padé approximants put a pole at $t=0$, without forcing it, clearly indicates the consistency of our approximations. Finally, in the Conclusion, we discuss, interpret, and compare our results to others for xenon, argon, and krypton atoms.

II. ANALYTIC PROPERTIES OF THE SCATTERING AMPLITUDES IN THE MOMENTUM-TRANSFER PLANE AT FIXED ENERGY

We consider the scattering of electrons of a few hundred electron volt energy by neutral atoms, viz. Xe, Kr, Ar. The target atoms are initially prepared in an $(L=S=0)$ state and then excited by electron impact to $(L=1,\ S=\frac{1}{2})$ state. The mass of the target atom is assumed to be infinite, and this will increase the analyticity domain, in the transfer t, of the scattering amplitude, by suppressing the right-hand cut. The scattering is represented by the reaction

$$e+A\rightarrow e+A^*\ , \tag{4}$$

where A^* is the atom in its final excited state; namely, we consider the following reactions [9–11]:

$$e+\mathrm{Xe}[5p^6(^1S_0)]\rightarrow e+\mathrm{Xe}[5p^5(^2P_{1/2,3/2})6s]\ , \tag{5}$$

$$e+\mathrm{Kr}[4p^6(^1S_0)]\rightarrow e+\mathrm{Kr}[4p^5(^2P_{1/2,3/2})5s]\ , \tag{6}$$

$$e+\mathrm{Ar}[3p^6(^1S_0)]\rightarrow e+\mathrm{Ar}[3p^5(^2P_{1/2,3/2})4s]\ . \tag{7}$$

Let $\mathbf{k}_i$ and $\mathbf{k}_f$ be the initial and final momenta of the electron projectile. The electron impact energy is defined by

$$E=\tfrac{1}{2}k_i^2=\tfrac{1}{2}k_f^2+\omega\ , \tag{8}$$

while the squared momentum transfer is given by

$$t=K^2=(\mathbf{k}_i-\mathbf{k}_f)^2=2E(1+x^2-2xy)\ , \tag{9}$$

where

$$x=\sqrt{1-\omega/E}\ ,\quad 0\le x<+1 \tag{10}$$

$$y=\cos\theta\ . \tag{11}$$

The physical range of t is from $t_{\min}$ to $t_{\max}$, viz.,

$$t_{\min}\le t\le t_{\max} \tag{12}$$

with

$$t_{\min}=2E(1-x^2)\ , \tag{13}$$

$$t_{\max}=2E(1+x^2)\ . \tag{14}$$

We see that $t=0$ can only be reached for $x=1$, that is at E equal to infinity, then $t_{\max}$ is of the order of $8E$.

At any fixed energy E, $t=0$ is always unphysical, and consequently an interpolation-extrapolation formula is necessary to reach it from the experimental data. It is clear that to define a *sensible* extrapolation to unphysical values the analytic properties of the quantities of interest are of crucial importance. The generalized oscillator strength (in a.u.) is defined by

$$F(t)=\frac{\omega}{2}\frac{k_i}{k_f}t\frac{d\sigma}{d\Omega}=\frac{\omega}{2}\frac{\alpha^2}{x}\bar{t}\frac{d\sigma}{d\Omega}\ , \tag{15}$$

where $d\sigma/d\Omega$ is the inelastic differential cross section, with

$$\bar{t}=\frac{t}{\alpha^2}\ ,\quad \alpha=\sqrt{2I}+\sqrt{2(I-\omega)}\ , \tag{16}$$

and I being the ionization potential of the target atom. The optical oscillator strength is defined by

$$\mathcal{S}_{\text{OOS}}=\lim_{t\to 0}F(t)=\frac{\omega}{2}\frac{\alpha^2}{x}\gamma\ , \tag{17}$$

where γ is the *residue* of $d\sigma/d\Omega$ at $t=0$. This last remark will be the root of this paper.

Analytic structure of the scattering amplitudes

The differential cross section is given in terms of the scattering amplitude $f(E,t)$ by

$$\frac{d\sigma}{d\Omega}=\frac{k_f}{k_i}|f(E,t)|^2=\frac{k_f}{k_i}f(E,t)f^*(E,t)\ , \tag{18}$$

where the $*$ operation corresponds to complex conjugation. From the analytic properties of $f(E,t)$ in the complex t plane, one deduces immediately the analytic properties of $f^*(E,t^*)$, the analytic Hermitian associate. The domain of analyticity of $f^*(E,t^*)$ is just the symmetric region with respect to the real axis to that of $f(E,t)$. As we shall show that $f(E,t)$ is analytic in the t plane deprived from the real negative axis, it results from the previous remark that $f^*(E,t^*)$ enjoys the same property. Therefore, defining the analytic extension of the differential cross section in the complex t plane by

$$\frac{d\sigma}{d\Omega}=\frac{k_f}{k_i}f(E,t)f^*(E,t^*)\ , \tag{19}$$

which of course reduces for real t to the physical formula Eq. (18), we see that the differential cross section will be analytic in the complex t plane less a cut from $-\infty$ to 0. To find the analytic properties of the amplitudes $f(E,t)$, we refer the reader to the model independent results of the theory of dispersion relations [19].

Previously Gerjuoy and Krall [20,21] analyzed atomic scattering problems using *energy* dispersion relations in contradistinction with the present work which makes use of *momentum*-transfer dispersion relations. Those authors were followed in their *energy* dispersion relations analysis by Rubin, Sugar, and Tiktopoulos [22] and Tip [23]. They have studied the amplitudes for breakup of a two-particle bound state and have shown that the amplitudes satisfy a dispersion relation in the energy for fixed values of the scattering angle. Again this contrasts with our approach where the relationships involve unphysical scattering angles but physical energies.

While additional poles and branch cuts are introduced in atomic physics due to the composite nature of the target and because of electron exchange, when one deals with *energy* dispersion relations, no such singularities and associated difficulties are expected when writing *momentum-transfer* dispersion relations. This is so because in the momentum-transfer channel besides the photon only very heavy particles can be exchanged, and taking into account the infinite mass approximation for the atoms, there would be no singularities in the *momentum-transfer complex plane* except the singularity linked to the photon itself.

It is known since the work of De Alfaro and Regge [24] that the Mandelstam representation is valid in the nonrelativistic limit. For our purpose this reduces to the fact that $f(E,t)$ is analytic in the full complex t plane less two cuts running on the real axis:

(i) A left-hand cut corresponding to $t\leq 0$. This cut is linked physically to the exchange of a photon of zero mass in the crossed channel reaction $e+\bar{e}\to A+\bar{A}$, where the bar corresponds to the antiparticle.

(ii) A right-hand cut running along the positive real t axis from

$$t=4\frac{M}{m}E\quad\text{to}\quad+\infty\ . \tag{20}$$

Here M is the atom mass, m that of the electron, while E is the electron impact energy in the rest frame system of the target atom. Physically, this cut comes from the exchange of an ionized atom of mass $M-m$ in the crossed channel of the reaction $\bar{e}+A\to\bar{e}+A$. In the limiting case where $M/m\to\infty$, which corresponds to the present situation, this cut recesses to infinity and is no longer present. Consequently, our cross sections are reduced to analytic functions with only the left-hand cut as stated. We note the following:

(i) Although our previous discussion dealt with the elastic process,

$$e+A\to e+A\ , \tag{21}$$

the same reasoning applies equally well to the inelastic process

$$e+A\to e+A^*\ . \tag{22}$$

(ii) The reader may be puzzled by the fact that we have used relativistic field theory arguments to get the analytic properties of the scattering amplitudes. This is not necessary at all; it was just a matter of convenience to use them, because all the work done on analyticity originated in field theory. For a pure nonrelativistic approach, use [19]. We end this section by giving the integral form of the dispersion relation for $f(E,t)$

$$f(E,t)=\int_0^\infty\frac{\rho(E,\mu)}{t+\mu^2}d\mu\ . \tag{23}$$

If we suppose that $\rho(E,\mu)$ has a finite limit when $\mu \to 0$, viz. $\rho(E,0)$, then from Eq. (23), for small t, $f(E,t)$ behaves as

$$\frac{\pi}{2}\frac{\rho(E,0)}{\sqrt{t}} . \tag{24}$$

This is best seen by making in Eq. (23) the change of variable $\mu=\hat{\mu}\sqrt{t}$. As a consequence of Eq. (24), the differential cross section behaves as

$$\frac{k_f}{k_i}\frac{\pi^2}{4}\frac{|\rho(E,0)^2|}{t} \quad \text{[optical theorem]} \tag{25}$$

and, combining Eq. (25) with Eq. (17), we find that the OOS is equal to

$$\frac{\omega}{2}\left[\frac{\alpha\pi}{2}\right]^2 |\rho(E,0)^2| . \tag{26}$$

We see that the Lassettre theorem implies that $\rho(E,0)$ be independent of E, because the OOS is supposed to be independent of E. Notice that the Lassettre theorem, or equivalently, the existence and the independence of $\rho(E,0)$ on E, results simply from the assumption of the pole dominance of the single photon exchange in the t crossed channel, combined with the p-wave dominance of the production process of the excited atom. The presence of a certain amount of s wave in the inelastic process will translate itself into a change of the computed GOS by a mechanism we shall explain in a forthcoming paper. In this approach, we shall ignore such a possibility.

III. THE PADÉ APPROXIMATION

Given a function $F(t)$, this could be for instance the scattering amplitude at fixed energy, the cross section at fixed energy, or the GOS, analytic in a cut plane and satisfying a dispersion relation

$$F(t)=\int_0^\infty \frac{\rho(\xi)}{t+\xi}d\xi . \tag{27}$$

We want to approximate it by a set of the most suitable rational fractions, that is a ratio of two polynomials in t. From the mathematical point of view, this is justified because the most complicated types of singularities, besides poles that are already embedded by construction in the approximation, can be represented. Essential singularities, poles of infinite order, can be approximated by a cluster of poles; logarithmic singularities by a sequence of poles along the cut associated with the singularity, etc.

From the physical point of view, Eq. (27) can be reinterpreted in an electrostatic analogy in the following way. We consider $\rho(\xi)$ as a linear electric density along the negative real axis and $F(t)$ as the electric potential generated by these charges at a point t in the complex plane. Keeping in mind this electrostatic analog, we shall use the principle of electric images to replace the continuous electric distribution $\rho(\xi)$ by a discrete one (point charges), and write for the approximate $F(t)$

$$F_d(t)=\int_0^\infty \left[\sum_{j=1}^{j=d}\rho_j\delta(\xi+\xi_j)\right]\frac{d\xi}{t+\xi} . \tag{28}$$

These d discrete charges sit on the left-hand cut at points $-\xi_j$ and have charges ρ_j. The net result for F_d is

$$F_d(t)=\sum_{j=1}^{j=d}\frac{\rho_j}{t+\xi_j}=\frac{P_{d-1}(t)}{Q_d(t)} , \tag{29}$$

where

$$Q_d(t)=\prod_{j=1}^{j=d}(t+\xi_j) \tag{30}$$

is a polynomial of degree d whose zeros are the $-\xi_j$. P_{d-1} is a polynomial of degree $d-1$. We see that this *electrostatic approach* produces naturally a rational fraction of degree $d-1$ at the numerator and degree d at the denominator.

The $2d$ unknowns $\{\rho_j,\xi_j\}_{j=1}^{j=d}$ are chosen in the following way: Given the values of $F(t)$ at the points of analyticity $t_1, t_2, \ldots, t_N$; that is,

$$F(t_k)=F_k , \quad k=1,2,\ldots,N , \tag{31}$$

we can impose these constraints to compute the ρ_j and the ξ_j. Using Eq. (29), we get the set of equations

$$F_k=\sum_{j=1}^{j=d}\frac{\rho_j}{t_k+\xi_j} \quad k=1,2,\ldots,N . \tag{32}$$

If we choose $N=2d$, we will get a set of N equations with N unknowns. Unfortunately, the system Eq. (32) is nonlinear and untractable. We now briefly describe a method inspired from the classical work of Stieltjes [16], by extending it to Padé approximants of type II, defined by the continued fraction

$$F_N(t)=\phi_1+\cfrac{t-t_1}{\phi_2+\cfrac{t-t_2}{\phi_3+\cfrac{t-t_3}{\ddots\;+\cfrac{\quad}{\phi_{N-2}+\cfrac{t-t_{N-2}}{\phi_{N-1}+\cfrac{t-t_{N-1}}{\phi_N}}}}}} \tag{33}$$

Depending on whether N is even or odd, $F_N(t)$ is a rational fraction of degree $[N/2]$ for the numerator and of degree $[(N-1)/2]$ for the denominator.[1] We shall fit the set $\{\phi_k\}_{k=1}^N$ by requiring that

$$F_N(t_k)=F_k , \quad k=1,2,\ldots,N . \tag{34}$$

$F_N(t)$ is called the Padé approximation of type II built on $F(t)$. This approximation enjoys deep and remarkable properties; the interested reader can refer to [16,17]. To compute easily the set $\{\phi_k\}_{k=1}^N$ from the knowledge of the set $\{F_j=F(t_j)\}_{j=1}^N$, we introduce the set of linear

[1]The notation $[x]$ means integer part of x.

fractional transformations

$$F_s(t)=\phi_{N-s+1}+\frac{t-t_{N-s+1}}{F_{s-1}(t)} \tag{35}$$

or, equivalently, by inverting Eq. (35)

$$F_{s-1}(t)=\frac{t-t_{N-s+1}}{F_s(t)-\phi_{N-s+1}} . \tag{36}$$

To initialize the system, we put

$$F_1(t)=\phi_N . \tag{37}$$

One checks that this set of transformations with Eq. (37) correctly generates Eq. (33). Setting $t=t_p$ in Eq. (35) gives

$$\phi_p=F_{N-p+1}(t_p) , \quad p=1,2,\ldots,N . \tag{38}$$

We now calculate explicitly the ϕ's, beginning with

$$F_N(t_1)=F_1 ; \quad F_N(t_2)=F_2 ; \quad \ldots ; F_N(t_N)=F_N , \tag{39}$$

which from Eq. (38) allows the immediate computation of

$$\phi_1=F_N(t_1)=F_1 . \tag{40}$$

Then we compute

$$F_{N-1}(t)=\frac{t-t_1}{F_N(t)-\phi_1}=\frac{t-t_1}{F_N(t)-F_1} . \tag{41}$$

This gives all $F_{N-1}(t_k)$ with $k=2,\ldots,N$, viz.,

$$F_{N-1}(t_2)=\frac{t_2-t_1}{F_2-F_1} ,$$

$$F_{N-1}(t_3)=\frac{t_3-t_1}{F_3-F_1} ,$$

$$\vdots$$

$$F_{N-1}(t_N)=\frac{t_N-t_1}{F_N(t)-F_1} , \tag{42}$$

and in particular

$$\phi_2=F_{N-1}(t_2)=\frac{t_2-t_1}{F_2-F_1} . \tag{43}$$

Continuing in this way, we can compute

$$F_{N-s}(t_{s+1}) ; \quad F_{N-s}(t_{s+2}) ; \quad \ldots ; \quad F_{N-s}(t_N) , \tag{44}$$

$$\phi_{s+1}=F_{N-s}(t_{s+1}) \tag{45}$$

and finally get

$$\phi_N=F_1(t_N) . \tag{46}$$

This elegant procedure allows the computation of the essential rational fraction that will fit the given analytic function.

IV. POLES AND ZEROS

A. Construction of the numerator and the denominator of the Padé approximations

In the previous section, we gave a scheme for expanding $F(t)$ in a continued fraction characterized by a set of ϕ's. The truncated (at order N) continued fraction $F_N(t)$ is defined by a subset of $\phi:\{\phi_k\}_{k=1}^N$, and we have learned how to compute the ϕ_k from the input data. One checks immediately that F_N is a rational fraction that we write for convenience as

$$F_N(t)=\frac{P_N(t)}{Q_N(t)} , \tag{47}$$

where $P_N(t)$ is a polynomial of degree $[N/2]$ and $Q_N(t)$ is a polynomial of degree $[(N-1)/2]$. Note that the index N is not the degree of the polynomials but a label indexing the order of the approximation.

Using the linear fractional transformation Eq. (35), it is not difficult to show that the polynomials $P_N(t)$ and $Q_N(t)$ satisfy the same three-term recursive relation involving only the knowledge of the ϕ's

$$R_k(t)=\phi_k R_{k-1}(t)+(t-t_{k-1})R_{k-2}(t) , \tag{48}$$

where $R_k(t)$ is either $P_N(t)$ or $Q_N(t)$. Only the initial conditions are different for the P's and the Q's. For the P's one has

$$P_1(t)=\phi_1 ,$$

$$P_2(t)=t+(\phi_1\phi_2-t_1) ,$$

$$\vdots$$

$$P_k(t)=\phi_k P_{k-1}(t)+(t-t_{k-1})P_{k-2}(t) , \tag{49}$$

while for the Q's, the relations are

$$Q_1(t)=1 ,$$

$$Q_2(t)=\phi_2 ,$$

$$\vdots$$

$$Q_k(t)=\phi_k Q_{k-1}(t)+(t-t_{k-1})Q_{k-2}(t) . \tag{50}$$

From these relations, one constructs immediately the recursive relations for the coefficients of the polynomials $P_k(t)$ and $Q_k(t)$, namely,

$$P_k(t)=p_k^{[k/2]}t^{[k/2]}+p_k^{[k/2]-1}t^{[k/2]-1}+\cdots +p_k^{[k/2]-l}t^{[k/2]-l}+\cdots+p_k^0 , \tag{51}$$

$$Q_k(t)=q_k^{[(k-1)/2]}t^{[(k-1)/2]}+q_k^{[(k-1)/2]-1}t^{[(k-1)/2]-1}+\cdots+q_k^{[(k-1)/2]-l}t^{[(k-1)/2]-l}+\cdots+q_k^0 . \tag{52}$$

One checks that

$$p_{2k}^k=q_{2k}^k=1 , \tag{53}$$

and

TABLE I. Noisy poles and zeros, corresponding to the electron-xenon elastic scattering at 100 eV, coming from experimental errors.

	Real part	Imaginary part
zero	0.011 376 530 307 507 876 1	0.000 000 000 000 000 000 0
pole	0.011 322 829 961 303 061 0	0.000 000 000 000 000 000 0
zero	0.051 199 228 528 817 482 3	0.009 464 864 297 820 334 28
pole	0.051 645 615 778 119 186 0	0.009 275 091 687 547 080 97
zero	0.051 199 228 528 817 482 3	−0.009 464 864 297 820 334 28
pole	0.051 645 615 778 119 186 0	−0.009 275 091 687 547 080 97

$$p_k^m=\phi_k p_{k-1}^m+p_{k-2}^{m-1}-t_{k-1}p_{k-2}^m \quad m=0,1,\ldots,[k/2]\ , \tag{54}$$

with an analogous recursive relation for q_k^m.

The initial conditions for the coefficients are derived from the knowledge of the first polynomials P_1, P_2, and Q_1, Q_2

$$p_1^0=\phi_1\ ,\quad p_2^1=1\ ,\quad p_2^0=\phi_1\phi_2-t_1\ , \tag{55}$$

and

$$q_1^0=1\ ,\quad q_2^0=\phi_2\ . \tag{56}$$

It is therefore possible to compute the coefficients of $P_k(t)$ and $Q_k(t)$ from the input values. The computer decimal precision required for these calculations is conservatively $2N$ decimal places, where N is the number of input data.

B. Poles and zeros structure

In the previous section, we have seen how to construct explicitly from the data the numerator and the denominator of the Padé approximation. We can rewrite Eq. (47) as

$$F_N(t)=K_N\prod_{l=1}^{[N/2]}(t-z_l^N)\Big/\prod_{l=1}^{[(N-1)/2]}(t-p_l^N)\ , \tag{57}$$

where the z's and the p's are the zeros and the poles of the Padé approximation, respectively, and K_N is given by

$$K_N=\begin{cases}[\phi_2+\phi_4+\cdots+\phi_N]^{-1} & \text{if } N \text{ is even}\ ,\\ [\phi_1+\phi_3+\cdots+\phi_N] & \text{if } N \text{ is odd}\ .\end{cases} \tag{58}$$

To find out the pattern of the poles and zeros, let us discuss a practical case extracted from the present case, rather than a theoretical discussion which can be found in [18]. We consider the elastic cross section for Xe at 100 eV. From the 14 nearest values of $K^2=0$, of the elastic differential cross section, one computes the Padé approximation $F_{14}(t)$ which is a rational fraction of degree seven at the numerator and degree six at the denominator or [7/6] approximation. We have therefore seven zeros and six poles to describe it, with one pole at infinity. The six poles and seven zeros have been, for the reader's convenience, split into three different families, represented in Tables I, II, and III. In Table I, we see three pairs of doublets pole zero whose inner relative distance is of the order of 0.5–2 %. Clearly these doublets represent the error due to the experimental data which are themselves of this magnitude.

In Table II, we see again three pairs of doublets pole zero whose inner relative distance is this time of the order of 10^{-13}. This corresponds to the noise generated by the computer roundoff. We have added for convenience a fictitious pole at infinity in Table II to compensate for the zero at 0.587×10^{26}. Finally, in Table III, what is left is the filtered pole and zero after the various polluting sources of noise have been taken away. This very powerful filtering is obtained through the explicit use of the analytic properties of the cross sections; without them, no such filtering could exist. Although it is not the proper place here to discuss the properties of the Padé approximations as analytic noise filter [18], let us very briefly sketch the origin of such properties. When an analytic function is measured experimentally, one picks up noise which is represented by a function $n(t)$. Therefore, the function one analyzes is no longer $F(t)$ but $\hat{F}(t)=F(t)+n(t)$. Because $n(t)$ presents natural boundaries in the complex t plane, that is, sets of dense singularities along some curves, $\hat{F}(t)$ will inherit them. The Padé approximations will tend to reproduce these natural

TABLE II. Noisy poles and zeros, corresponding to the electron-xenon elastic scattering at 100 eV, coming from computer roundoff. The numbers in brackets denote multiplicative powers of ten.

	Real part	Imaginary part
zero	0.029 393 737 442 456 349 0	0.341 535 222 086 635 176[−03]
pole	0.029 393 737 442 448 639 9	0.341 535 222 093 373 764[−03]
zero	0.029 393 737 442 456 349 0	−0.341 535 222 086 635 176[−03]
pole	0.029 393 737 442 448 639 9	−0.341 535 222 093 373 764[−03]
zero	0.587 392 030 111 528 023[+26]	0.000 000 000 000 000 000
pole	Infinity	0.000 000 000 000 000 000

TABLE III. Filtered poles and zeros, corresponding to the electron-xenon elastic scattering at 100 eV.

	Real part	Imaginary part
zero	−1.276 972 042 685 660 34	0.000 000 000 000 000 000
pole	−0.018 386 108 761 050 356 4	0.000 000 000 000 000 000

boundaries also. It can be shown that they are represented by doublets of pole zero with an inner distance of the order of the noise. We can now get a clean representation for the quantity $F(t)$. Instead of Eq. (57), we shall now have

$$\bar{F}_N(t)=K_N \prod_{l=1}^{[N/2]-n}(t-z_l^N)\Big/\prod_{l=1}^{(N-1)/2]-n}(t-p_l^N)\ , \tag{59}$$

where we have discarded n pole-zero doublets corresponding to the noise. $\bar{F}(t)$ is the analytically filtered version of $F(t)$. For the previous example, we get

$$\sigma(t)=\hat{K}_{14}\frac{t-z_t}{t-p_t}\ , \tag{60}$$

where z_t and p_t stand for the true zero and true pole given in Table III, and $\hat{K}_{14}$ has the value

$$\hat{K}_{14}=K_{14}(t-t_L)\ . \tag{61}$$

Using Eq. (58) gives us the value of K_{14}, that is,

$$K_{14}=-0.7615\times 10^{-25} \tag{62}$$

and t_L is the largest zero value in Table II. Neglecting the value of t with respect to that of t_L, we get $\hat{K}_{14}=4.473$.

Finally, let us make two more remarks before closing this section.

(i) For large t the cross section tends to zero; none of the Padé approximations tend to zero for large t: the even ones tend to infinity like, $K_N t$ while the odd ones tend to the constant K_N. It is easy to circumvent this difficulty and construct approximations that will behave correctly, that is, tend to zero for large t. A simple way is to construct the Padé approximations to the inverse function of interest, namely the Padé of $1/F$ rather than that of F. Then the even approximations to $1/F$ will go to infinity proportionally to t and their inverse will go to zero like $1/t$. We shall also make use of this remark to compute the OOS.

(ii) We can compute $\hat{K}_{14}$ in a different way, using a best-fit procedure. We introduce the error functional

$$E(\hat{K}_{14})=\sum_{i=1}^{i=14}\left[\sigma(t_i)-\hat{K}_{14}\frac{t_i-z_t}{t_i-p_t}\right]^2\ . \tag{63}$$

Minimizing this functional with respect to $\hat{K}_{14}$, we get

$$\hat{K}'_{14}=\sum_{i=1}^{i=14}\sigma(t_i)\frac{t_i-z_t}{t_i-p_t}\Big/\sum_{i=1}^{i=14}\left[\frac{t_i-z_t}{t_i-p_t}\right]^2\ . \tag{64}$$

We can now compare this value with the value of $\hat{K}_{14}$ following Eq. (62), viz.

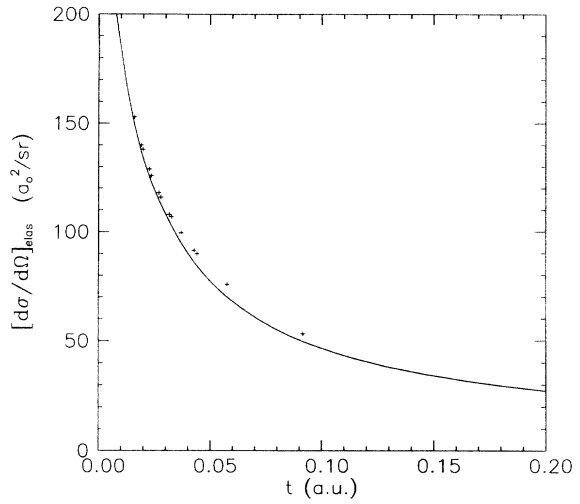

FIG. 2. Elastic differential cross sections for Xe at 100 eV. The current filtered result (solid line) is compared with the Suzuki *et al.* [9] (crosses) data.

$$\hat{K}'_{14}=4.473\ . \tag{65}$$

There is an excellent agreement between the value of $\hat{K}_{14}$ and $\hat{K}'_{14}$.

V. OOS CALCULATION AND CONCLUSION

In Figs. 2 and 3, we give examples of the use of the Padé approximation in the interpolation-extrapolation and the filtering of experimental data. In particular, in Fig. 2 while we input 14 experimental data for elastic differential cross section for xenon atom at 100 eV the filtered Padé approximant (sold curve) depends only on *three* parameters [see Eq. (60)]. In Fig. 2 the solid curve

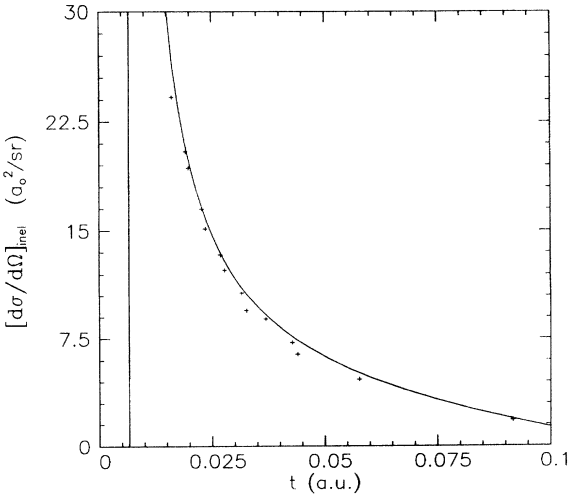

FIG. 3. Inelastic differential cross section corresponding to the $5p^6(^1S_0)\rightarrow 5p^5(^2P_{1/2})6s$ transition versus K^2 (a.u.) at 100 eV for xenon atom. The current filtered result (solid line) is compared with the Suzuki *et al.* [9] (crosses) result.

represents our filtered result for the elastic differential cross section for Xe at 100 eV, while the crosses are the Suzuki *et al.* [9] data. Figure 3 compares the filtered (solid curve) and the experimental (crosses) data for the Xe $5p^6(^1S_0)\rightarrow 5p^5(^2P_{1/2})6s$ transition at 100 eV. This dramatic reduction in the number of parameters as well as the quality of the fit shows the power and efficiency of the method. It must be pointed out that those Padé approximants satisfy, by construction, all the constraints implied by the momentum-transfer dispersion relations representation.

As our main goal, we have computed the residue of the true pole nearest to the origin in the Padé approximation to the differential cross section. The optical oscillator strength (OOS) is then proportional to it within a simple kinematical factor. The fact that the method does *not* by construction put a pole at $t=0$, but produces it, is a crucial feature of our method. Let us discuss briefly the case of Xe at 100 eV. In this case, for the inelastic cross section, the pole in the $J=\frac{1}{2}$ state is found at $t=0.006$, while for $J=\frac{3}{2}$, the pole sits at $t=0.0025$. The value $t=0.0025$ is certainly compatible within the experimental errors with zero, and therefore confirms the hypothesis of p-wave dominance. This result is supported by the fact that for $J=\frac{3}{2}$, the optical measurements are in reasonable agreement with the extrapolated OOS from electron scattering data, as can be seen from Tables IV, V, and VI. The (i) values of the OOS are related to the residue of the true pole of the Padé approximation whereas the (ii) values are related to a more standard approximation, *forcing the pole to be zero.*

The pole at $t=0.006$ in the $J=\frac{1}{2}$ state, is farther away from the origin than its sibling in the $J=\frac{3}{2}$ state. This is a rather general situation; for krypton at 500 eV, this is even more striking, the pole at $J=\frac{1}{2}$ is found to be at

TABLE IV. Comparison of the optical oscillator strength for xenon atom, with other results. The fourth column lists the ratio of the $^2P_{3/2}$ strength to the $^2P_{1/2}$ strength.

Author	OOS $^2P_{1/2}$	OOS $^2P_{3/2}$	Ratio
	Semiempirical		
This work	(i) 0.141±0.019	0.208±0.027	1.10
	(ii) 0.164±0.019	0.223±0.027	1.36
	EELS		
Suzuki *et al.*[a]	0.158±0.019	0.222±0.027	1.41
Lu[b]	0.189	0.272	1.44
Geiger[c]	0.19	0.260	1.37
Delage and Carette	0.169	0.183	1.08
Brion[e]	0.173	0.252	1.46
	Optical measurements		
Anderson[f]	0.238	0.256	1.08
Wilkinson[g]	0.260	0.270	1.04
	Calculations		
Dow and Knox[h]	(A) 0.147	0.194	1.32
	(B) 0.170	0.190	1.12
Kim *et al.*[i]	0.189	0.212	1.12

[a]Reference [9].
[b]Reference [25].
[c]Reference [26].
[d]Reference [27].
[e]Reference [28].
[f]Reference [29].
[g]Reference [30].
[h]Reference [31].
[i]Reference [32].

TABLE V. Comparison of the optical oscillator strength for argon atom, with other results.

Author	OOS $^2P_{1/2}$	OOS $^2P_{3/2}$
	Semiempirical	
This work	(i) $0.222^{+0.02}_{-0.03}$	$0.04547^{+0.005}_{-0.008}$
	(ii) $0.2168^{+0.02}_{-0.03}$	$0.0469^{+0.005}_{-0.008}$
	EELS	
Li *et al.*[a]	$0.222^{+0.02}_{-0.03}$	$0.058^{+0.005}_{-0.008}$
Chamberlain *et al.*[b]	0.181	0.049
	Optical measurements	
Lawrence[c]	0.228±0.021	0.059±0.003
Stacey and Vaughan[d]	0.275±0.02	0.036±0.004
Lewis[e]	0.278±0.002	
de John and van Eck[f]	0.22±0.02	
McConkey and Donaldson[g]		0.096±0.02
	Calculations	
Dow and Knox[h]	(A) 0.17	0.052
	(B) 0.20	0.049

[a]Reference [11].
[b]Reference [33].
[c]Reference [34].
[d]Reference [35].
[e]Reference [36].
[f]Reference [37].
[g]Reference [38].
[h]Reference [31].

TABLE VI. Comparison of the optical oscillator strength for krypton atom, with other results.

Author	OOS $^2P_{1/2}$	OOS $^2P_{3/2}$
	Semiempirical	
This work	(i) 0.127±0.015	0.1855±0.015
	(ii) 0.114±0.015	0.1124±0.015
	EELS	
Takayanagi *et al.*[a]	0.127±0.015	0.143±0.015
Geiger[b]	0.173±0.035	0.173±0.035
	Optical measurements	
Wilkinson[c]	0.159	0.135
de John and van Eck[d]	0.142±0.015	
Tsurubuchi *et al.*[e]	0.139±0.010	0.155±0.011
Lewis[f]	0.174	0.193
	Calculations	
Dow and Knox[g]	(A) 0.136	0.138
	(B) 0.153	0.152

[a]Reference [10].
[b]Reference [39].
[c]Reference [40].
[d]Reference [37].
[e]Reference [41].
[f]Reference [36].
[g]Reference [31].

$t=0.003\,79$, while in the $J=\frac{3}{2}$ channel, it sits at $t=0.000\,05$. The discrepancy in the OOS values, for the Xe $[5p^5(^2P_{1/2})6s]$ case, between optical measurements of Anderson [29] and Wilkinson [30] on the one hand, and other measurements and calculations, including ours, on the other hand, could simply indicate a *much more complicated structure of the analytic differential cross section near $t=0$, than a simple pole.* The way to analyze this structure will be the subject of a future investigation. In this paper we wanted only to introduce the matter of analytic interpolation-extrapolation of experimental data for atomic physics, that is, the use of *momentum-transfer dispersion relations* in atomic physics and firmly set the grounds for it.

Some remarks about the accuracy of the OOS in Tables IV, V, and VI are appropriate. For both Xe $[5p^5(^2P_{1/2})6s]$ and the Xe $[5p^5(^2P_{3/2})6s]$ states our values agree well with the Suzuki *et al.* measurement within the errors. Also, the electron-energy-loss-spectroscopy (EELS) measured OOS, except those of references [25] and [26], are centered around the Suzuki *et al.* data and are in reasonable agreement with the theoretical values [26,31]. However, both the optical measurements [29,30] are rather too high by comparison. Therefore, we believe that the Suzuki *et al.* OOS are close to the correct values. In the case of argon our results are in good agreement with the data of Li *et al.* [11] and within the errors, with the EELS data of Chamberlain *et al.* [33] as well as reasonably well with the calculations of Dow and Knox [31]. Among the optical measurements, agreement is only with Lawrence [34] and the de Jongh and van Eck [37] data. The remaining optical measurements [35,36] are too high, even when the errors are considered. We conclude that for argon, the correct OOS are probably those of Li *et al.* or there about.

For krypton Gieger [39], an EELS measurement, and Lewis [36], an optical measurement, both overestimate the OOS. All other measurements and calculations, including the current one, support the EELS measurements of Takayanagi *et al.* Puzzling in this case is that our OOS calculations (i) for $5p^5(^2P_{3/2})4s$ state is rather high even with the errors included. Nevertheless, the Takayanagi *et al.* measurements are probably close to the correct values.

In conclusion, we have introduced momentum-transfer dispersion in atomic physics, thus providing an alternative method to calculate OOS from differential cross sections. Our method being unbiased, general, model-independent, and based on the analytic properties of the scattering amplitude in the scattering angle, gives credence to the Suzuki *et al.*, Li *et al.*, and Takayanagi *et al.* fits and consequent analysis. The Chan *et al.* [42,43] measurements of OOS for argon, krypton, and xenon are much higher than the current theoretical and the above-mentioned experimental data.

ACKNOWLEDGMENTS

This work was supported by the National Science Foundation and DOE, Office of Basic Energy Sciences, Division of Chemical Sciences. Generous supercomputer time at NERSC, through DOE, Fusion Energy Research, and DOE Office of Basic Energy Sciences, Division of Chemical Sciences, is greatly appreciated.

[1] W. F. Miller and R. L. Platzman, Proc. R. Soc. London, Ser. A **70**, 229 (1957).
[2] E. N. Lassettre, A. Skerbele, and M. A. Dillon, J. Chem. Phys. **50**, 1829 (1969).
[3] S. M. Silverman and E. N. Lassettre, J. Chem. Phys. **40**, 1265 (1964).
[4] L. Vuskovic, S. Trajmar, and D. F. Register, J. Phys. B **15**, 2517 (1982).
[5] L. Vuskovic, L. Maleki, and S. Trajmar, J. Phys. B **17**, 2519 (1984).
[6] S. Trajmar, W. Williams, and S. K. Srivastava, J. Phys. B **10**, 3323 (1977).
[7] L. V. Hertel and K. J. Ross, J. Phys. B **2**, 285 (1969).
[8] K. N. Klump and E. N. Lassettre, J. Chem. Phys. **68**, 3511 (1978).
[9] T. Y. Suzuki, Y. Sakai, B. S. Min, T. Takayanagi, K. Wakiya, H. Suzuki, T. Inaba, and H. Takuma, Phys. Rev. A **43**, 5867 (1991).
[10] T. Takayanagi, G. P. Li, K. Wakiya, H. Suzuki, T. Ajiro, T. Inaba, S. S. Kano, and H. Takuma, Phys. Rev. A **41**, 5948 (1990), and references therein.
[11] G. P. Li, T. Takayanagi, K. Wakiya, H. Suzuki, T. Ajiro, S. Yagi, S. S. Kano, and H. Takuma, Phys. Rev. A **38**, 1240 (1988).
[12] A. Skerbele and E. N. Lassettre, J. Chem. Phys. Lett. **51**, 424 (1978).
[13] K. N. Klump and E. N. Lassettre, J. Chem. Phys. Lett. **51**, 99 (1977).
[14] A. Z. Msezane and R. J. W. Henry, Phys. Rev. Lett. **55**, 2277 (1985).
[15] R. H. Hansen, F. J. de Heer, H. J. Luyken, B. Van Wingerden, and H. Blaauw, J. Phys. B **9**, 185 (1976).
[16] G. A. Baker, Jr., *The Essential of Padé Approximations* (Academic, New York, 1975); J. L. Basdevant, D. Bessis, and J. Zinn-Justin, Nuovo Cimento Serie X **60A**, 185 (1969).
[17] G. A. Baker, Jr. and P. Graves-Morris, *Padé Approximants,* Encyclopedia of Mathematics and its Applications Vols. 13 and 14 (Addison-Wesley, Reading, MA, 1981), Vol. 13, p. 65.
[18] J. Gilewicz and B. Truong-Van, *Froissart Doublets in the Padé Approximation and Noise, in Constructive Theory of Functions* (Sofia, Bulgaria, 1988).
[19] M. L. Goldberger, in *Relation de Dispersion et Particules Elmentaires* (Hermann, Paris, 1960).
[20] E. Gerjuoy and N. Krall, Phys. Rev. **119**, 705 (1960).
[21] E. Gerjuoy and N. Krall, Phys. Rev. **127**, 2105 (1962).
[22] M. H. Rubin, R. L. Sugar, and G. Tiktopoulos, Phys. Rev. **162**, 1555 (1967).
[23] A. Tip, in *Invited Papers and Progress Reports of the Tenth International Conference on the Physics of Electronic and Atomic Collisions, Paris, 1977,* edited by G. Watel (North-

Holland, Amsterdam, 1977).
[24] V. De Alfaro and T. Regge, *Potential Scattering* (North-Holland, Amsterdam, 1965).
[25] K. T. Lu, Phys. Rev. A **4**, 579 (1971).
[26] J. Geiger, in *Proceedings of the Fourth International Conference on Vacuum Ultraviolet Radiation Physics, Hamburg, 1974,* edited by E. E. Koch, R. Haensel, and R. Hunz (Pergamon, New York, 1974), p. 28.
[27] A. Delage and J. D. Carette, Phys. Rev. A **14**, 1345 (1976).
[28] C. E. Brion, see [9] for further references.
[29] D. K. Anderson, Phys. Rev. A **137**, 21 (1965).
[30] P. G. Wilkinson, J. Quant. Spectros. Radiat. Transfer **6**, 823 (1966).
[31] J. D. Dow and R. S. Knox, Phys. Rev. A **152**, 50 (1966).
[32] Y. K. Kim, M. Inokuti, G. E. Chamberlain, and S. R. Mielczarek, Phys. Rev. Lett. **21**, 1146 (1968).
[33] G. E. Chamberlain, J. G. M. Heideman, J. A. Simpson, and C. E. Kuyatt, in *Abstracts in Proceedings of the Fourth International Conference on the Physics of Electronics and Atomic Collisions, Quebec, 1965,* edited by L. Kerwin and W. Fite (Science Bookcrafters, Hastings-on-Hudson, 1968).
[34] G. M. Lawrence, Phys. Rev. A **175**, 40 (1968).
[35] D. N. Stacey and J. M. Vaughan, Phys. Lett. **11**, 105 (1964).
[36] E. L. Lewis, Proc. Phys. Soc. London, Sect. A **92**, 817 (1967).
[37] J. P. de Jongh and J. Van Eck, Physica (Utrecht) **51**, 104 (1971).
[38] J. W. McConkey and F. G. Donaldson, Can. J. Phys. **51**, 914 (1973).
[39] J. Geiger, Phys. Lett. **33A**, 351 (1970).
[40] P. G. Wilkinson, J. Quant. Spectros. Radiat. Transfer **5**, 503 (1965).
[41] S. Tsurubuchi, K. Watanabe, and T. Arikawa, J. Phys. B **22**, 2969 (1989).
[42] R. W. Wagenaar, A. de Boer, T. van Tubergen, J. Los, and F. J. de Heer, J. Phys. B **19**, 3121 (1986).
[43] W. F. Chan, G. Cooper, X. Guo, G. R. Burton, and C. E. Brion, Phys. Rev. A **46**, 149 (1992).